Quantifying MR Properties of the Cirrhotic Liver Using Explanted Specimens

B. E. Chapman[1], J. W. Marsh[2], M. E. Tublin[1]

[1]Department of Radiology, University of Pittsburgh, Pittsburgh, PA, United States, [2]Department of Surgery, University of Pittsburgh, Pittsburgh, PA, United States

Introduction

As the incidence of liver disease increases world-wide, imaging the cirrhotic liver is an increasingly important radiological issue. Many important findings, such as early stage hepatocellular carcinomas (HCC), are very subtle and difficult to visualize. Rapid imaging of the liver would facilitate quantitative multispectral imaging techniques that have shown promise in other organ systems, notably the brain. However, MR imaging of the liver is challenging due to respiratory motion and field inhomogeneities. To determine the nature of the MR multispectral information in the cirrhotic liver, we have begun to use MR to evaluate explanted livers prior to the normal pathology routine. We report our preliminary experience with quantifying the MR properties of explanted livers.

Methods

We collect cirrhotic livers directly from the operating room and take them to the MR suite where imaging is commenced as soon as a magnet becomes available. Imaging is typically completed within several hours of the liver being removed from a transplant recipient. Initially, livers were imaged in air. However, this resulted in some prominent susceptibility artifacts. Later images were acquired with the liver partially submerged in an extracellular fluid to reduce the susceptibility artifact. All imaging has been performed on a GE 1.5T Signa scanner equipped with high performance gradients (40 mT/m peak gradient, 150 T/m/s slew rate). A liver is placed in the standard GE transmit/receive headcoil. The minimum field-of-view containing the liver ranges from 24 cm to 35 cm. We measured the following parameters: **T1:** T1 was measured following a technique advocated by Deoni et al [Deoni, Rutt, Peters, MRM 2003] where a GRE sequence was used with varying flip angle. We assumed a base T1 value of 500 ms. With a TR of 50 ms, the Ernst angle was 25 degrees. This flip angle was used to compute the receiver gains which were then fixed for subsequent acquisitions. A 3D (32 or 64 z phase encodes) interleaved (8 or 16) spiral acquisition was used with a minimum TE (5 ms) to minimize dephasing. Flip angles ranged from 5 to 75 degrees. **T2*:** T2* was quantified using a GRE spiral sequence with varying echo times. Matrix definitions matched those used for the T1 acquisition. The TR was increased to 80 ms to allow for a longer TE, and the flip angle was increased to 30 degrees to compensate for the longer TR. Echo times ranged from 5 ms to 45 ms. **T2:** Because we did not have a correctly functioning 180 degree refocusing pulse on the spiral sequence, two dual echo 2D FSE images were acquired with echo times of 14, 28, 84 and 98 ms. Contiguous 5 mm slices were acquired with a 256x256 in-plane matrix. **Fat:** We did a qualitative estimate of fat content by acquiring out-of-phase and in-phase 2D GRE images. Using estimates of T2* or (T2 if T2* unavailable) we corrected for signal loss due to the increased echo time. Normalized changes in signal intensity were taken as indicators of the presence or absence of fat in the tissue.

Results

We have to date done ex vivo imaging on ten explanted livers. Example T1, T2 and fat maps are shown in FIG. 1. To estimate the spatial variability of the measurements, the images were divided into 16x16x2 subregions for which the median value for each parameter was computed. FIG. 2 shows example scatter plots based on these subregion measurements for T1, T2 and Fat. T2* measurements were of questionable quality due to a large amount of blurring introduced in the spiral images by long echo times needed to trace out the decay curve. Seven HCC nodules were found in one subject positive for Hepatitis C. In addition to the subregion measurements, circular ROIs were centered on each of these tumors as well as a large (20 pixel radius) background region. Mean measurements for these ROIs are shown in Table 1.

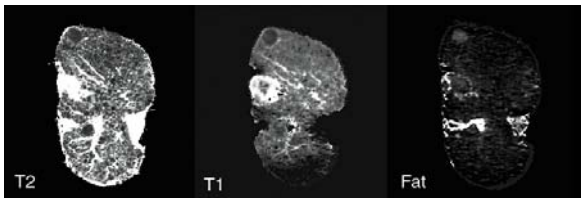

Fig. 1. Example parameter maps obtained on an explanted liver. Six HCC nodules were found in this liver of a patient positive for Hepatitis C.

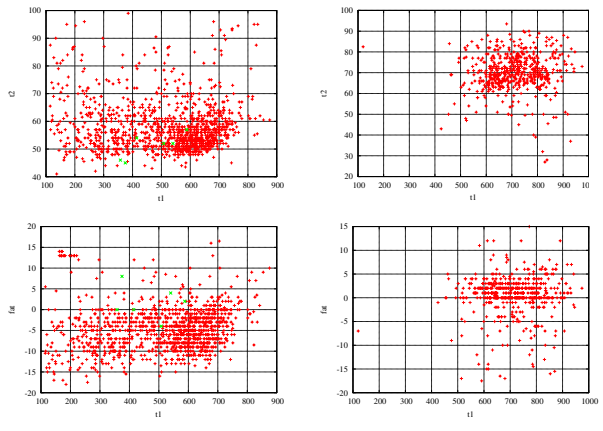

Fig. 2. Example scatter plots for the subregion measurements. The upper plots are T1/T2 plots, whereas the lower plots contain T1/Fat plots. The plots in the left column are from a Hepatitis C patient with 6 HCC nodules. The plots on the right are for a transplant recipient without Hepatitis C. Each mark represents the median value in a 16x16x2 region. ROIs containing HCC nodules are shown in green. The positive case showed considerably more spatial inhomogeneity than other livers.

Table 1. Mean and Standard Deviation MR Parameter Measurements for HCC Nodules

Sample	T1 in ms	T2 in ms	Fat % diff
Background	594	50	-8.43
	(84.0)	(7.6)	(6.9)
Tumor1	324	52.3	-1.38
	(79.9)	(7.0)	(5.9)
Tumor 2	338.34	47.6	-4.03
	(31.5)	(5.0)	(3.5)
Tumor 3	325.21	44.17	2.88
	(35.08)	(4.1)	(5.56)
Tumor 4	560	63	14
	(58.6)	(6.2)	(3.6)
Tumor 5	391	49.1	7.92
	(71.8)	(7.1)	(6.9)
Tumor 6	482.7	50.4	3.81
	(59.7)	(5.1)	(10.7)

Discussion

We have obtained preliminary quantification of several important MR parameters in the cirrhotic liver using explanted liver specimens. These measurements indicate that there is good separation between background tissue and HCC nodules in T1, with HCC's having a substantially smaller T1 value. There are also preliminary indications that fat is a useful mechanism for differentiating HCC nodules from the surrounding tissue. However, this may be of limited value in patients who have diffuse fatty infiltration. T2 values in the HCC nodules tend to be slightly lower than the surrounding background tissue and fat, but the amount of separation is small enough that combining the T1 and T2 values in a multispectral model is not likely to be beneficial. We are also examining the suitability of using other measures such as diffusion and magnetization transfer for the construction of multispectral models. Implementation of rapid quantitative imaging of the liver in vivo remains challenging. Respiration and static field inhomogeneities provide daunting challenges that must be overcome. We hope that our explanted imaging experience will provide useful guidelines for tackling the in vivo problem.